Chimera states in mechanical oscillator networks

Erik Andreas Martens[a,b,1,2], Shashi Thutupalli[c,d,1,2], Antoine Fourrière[c], and Oskar Hallatschek[a,e]

[a]Group of Biophysics and Evolutionary Dynamics and [c]Department of Dynamics of Complex Fluids, Max Planck Institute for Dynamics and Self-Organization, 37077 Göttingen, Germany; [b]Centre for Ocean Life, National Institute for Aquatic Resources, Technical University of Denmark, 2800 Kongens Lyngby, Denmark, [d]Departments of Physics and Mechanical and Aerospace Engineering, Princeton University, Princeton, NJ 08544; and [e]Department of Physics, University of California, Berkeley, CA 94720

Edited* by Boris I. Shraiman, University of California, Santa Barbara, CA, and approved May 10, 2013 (received for review February 14, 2013)

The synchronization of coupled oscillators is a fascinating manifestation of self-organization that nature uses to orchestrate essential processes of life, such as the beating of the heart. Although it was long thought that synchrony and disorder were mutually exclusive steady states for a network of identical oscillators, numerous theoretical studies in recent years have revealed the intriguing possibility of "chimera states," in which the symmetry of the oscillator population is broken into a synchronous part and an asynchronous part. However, a striking lack of empirical evidence raises the question of whether chimeras are indeed characteristic of natural systems. This calls for a palpable realization of chimera states without any fine-tuning, from which physical mechanisms underlying their emergence can be uncovered. Here, we devise a simple experiment with mechanical oscillators coupled in a hierarchical network to show that chimeras emerge naturally from a competition between two antagonistic synchronization patterns. We identify a wide spectrum of complex states, encompassing and extending the set of previously described chimeras. Our mathematical model shows that the self-organization observed in our experiments is controlled by elementary dynamical equations from mechanics that are ubiquitous in many natural and technological systems. The symmetry-breaking mechanism revealed by our experiments may thus be prevalent in systems exhibiting collective behavior, such as power grids, optomechanical crystals, or cells communicating via quorum sensing in microbial populations.

ensemble dynamics | statistical physics | nonlinear dynamics

In 1665, Christiaan Huygens observed that two pendulum clocks suspended on a beam always ended up swinging in exact antiphase motion (1) regardless of each pendulum's initial displacement. He explained this self-emergent synchronization as resulting from the coupling between the clocks, which was mediated by vibrations traveling across the beam. Huygens' serendipitous discovery has inspired many studies to establish that self-emergent synchronization is a central process to a spectacular variety of natural systems, including the beating of the heart (2), flashing fireflies (3), pedestrians on a bridge locking their gait (4), circadian clocks in the brain (5), superconducting Josephson junctions (6), chemical oscillations (7, 8), metabolic oscillations in yeast cells (9), and life cycles of phytoplankton (10).

Ten years ago, the dichotomy between synchrony and disorder was challenged by a theoretical study revealing that a population of identical coupled oscillators can attain a state where one part synchronizes and the other oscillates incoherently (11–23). These "chimera states" (13) emerge when the oscillators are coupled nonlocally (i.e., the coupling strength decays with distance between oscillators), which is a realistic scenario in many situations, including Josephson junction arrays (24) or ocular dominance stripes (25). Chimera states are counterintuitive because they occur even when units are identical and coupled symmetrically; however, with local or global coupling, identical oscillators either synchronize or oscillate incoherently but never do both simultaneously.

Since their discovery, numerous analytical studies (13, 14, 16–18) involving different network topologies (14, 19, 20) and various sources of random perturbations (21, 22) have established chimeras as a robust theoretical concept and suggest that they exist in complex systems in nature with nonlocal interactions. However, experimental evidence for chimeras has been particularly sparse so far, and it has only been achieved recently via computer-controlled feedback (26, 27). This raises the question of whether chimeras can only be produced under very special conditions or whether they arise via generic physical mechanisms. Uncovering such physical mechanisms requires analytically tractable experiments with direct analogs to natural systems.

Our mechanical experiment shows that chimera states emerge naturally without the need to fine-tune interactions. We implement the simplest form of nonlocal coupling that can be achieved using a hierarchical network with two subpopulations (14, 15): Within each subpopulation, oscillators are coupled strongly, whereas the coupling strength between the two subpopulations is weaker. We place N identical metronomes (28) with a nominal beating frequency f on two swings, which can move freely in a plane (Fig. 1 and Figs. S1–S3). Oscillators within one population are coupled strongly by the motion of the swing onto which the metronomes are attached. As f is increased, more momentum is transferred to the swing, effectively leading to a stronger coupling among the metronomes. A single swing follows a phase transition from a disordered state to a synchronized state as the coupling within the population increases (28, 29). This mimics the synchronization of the gait of pedestrians on the Millennium Bridge (4) wobbling under the pedestrians' feet. In our setup, emergent synchronization can be perceived both aurally (unison ticking) and visually (coherent motion of pendula). Finally, the weaker coupling between the two swings is achieved by tunable steel springs with an effective strength κ.

Results

For nonzero spring coupling, $\kappa > 0$, we observe a broad range of parameters in which chimeras (Fig. 1*C* and Movie S1) and further partially synchronized states emerge. To explore this complex behavior quantitatively, we measure the metronomes' oscillation phase θ_k, their average frequencies $\overline{\omega_k}$, and the complex order parameter $Z_p(t) = N^{-1}\sum_{k=1}^{N} e^{i[\theta_k^{(p)}(t) - \overline{\theta}_{\mathrm{syn}}(t)]}$, where $p = 1, 2$ denotes the left or right population and $\overline{\theta}_{\mathrm{syn}}$ is the average phase of the synchronous population ($|Z|$ quantifies the degree of synchronization: $|Z| \approx 0$ for incoherent motion and $|Z| \approx 1$ for synchronous motion).

Author contributions: E.A.M., S.T., and O.H. designed research; E.A.M., S.T., and A.F. performed research; E.A.M., S.T., and A.F. contributed new reagents/analytic tools; E.A.M. and S.T. analyzed data; E.A.M., S.T., A.F., and O.H. discussed the results and commented extensively on the manuscript at all stages of preparation; and E.A.M., S.T., and O.H. wrote the paper.

The authors declare no conflict of interest.

*This Direct Submission article had a prearranged editor.

Freely available online through the PNAS open access option.

[1]E.A.M. and S.T. contributed equally to this work.

[2]To whom correspondence may be addressed. E-mail: erik.martens@ds.mpg.de or shashi@princeton.edu.

This article contains supporting information online at www.pnas.org/lookup/suppl/doi:10.1073/pnas.1302880110/-/DCSupplemental.

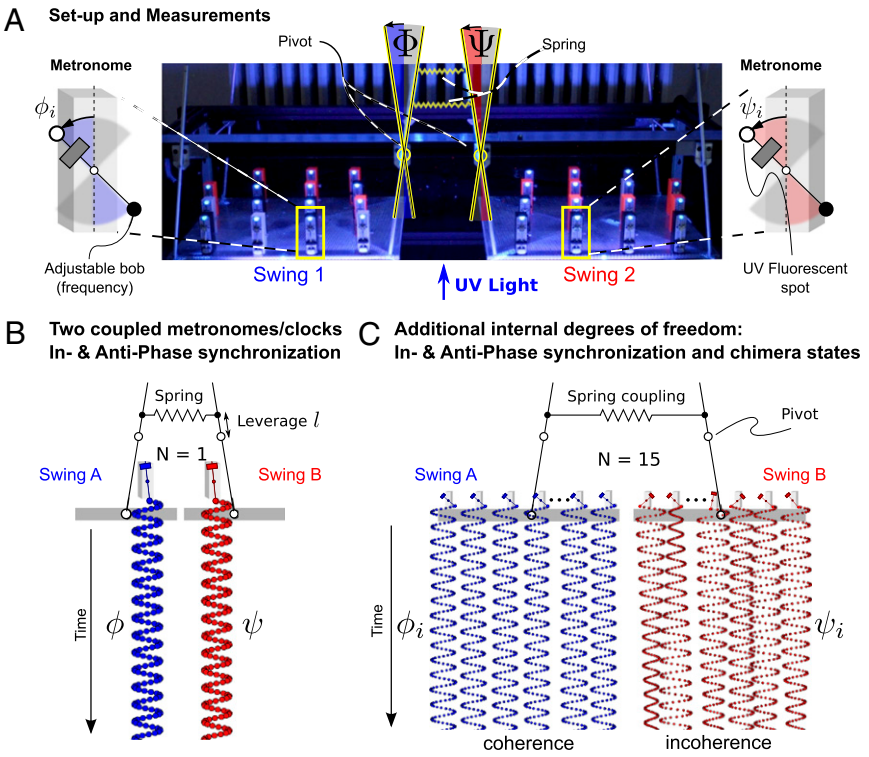

Fig. 1. Experimental setup and measurements. Two swings are loaded with N metronomes each and coupled with adjustable springs. (*A*) Swing and metronome displacements are measured by digital tracking of UV fluorescent spots placed on the pendula and swings. (*B*) $N = 1$: Metronomes synchronize in AP or IP motion. (*C*) $N = 15$: Symmetry-breaking chimera states with one metronome population synchronized and the other desynchronized, or vice versa. The displacement angles of the pendula on the left and right swings are ϕ_i and ψ_i, respectively.

To investigate where chimeras emerge in parameter space, we have systematically varied the effective spring coupling, κ, and the nominal metronome frequency, f, while ensuring that the metronomes on uncoupled swings synchronize. The long-term behavior of the system is studied by preparing the experiments with several initial conditions (*SI Text*) (12–14): (*i*) Both populations are desynchronized [desync-desync (DD)], or (*ii*) one population is synchronous and the other is desynchronized [sync-desync (SD) and desync-sync (DS), respectively]. We start with a fixed frequency and gradually decrease κ. For sufficiently large κ, the spring is effectively so stiff that the two swings act like one and metronomes evolve to a synchronized in-phase (IP) motion, such that the complex order parameters overlap with $|Z_{1,2}| \approx 1$ (Fig. 2*A* and Movie S2). For low κ, we observe that the two metronome populations settle into synchronized antiphase (AP) motion, where the order parameters and phases are separated in the complex plane by 180° with $|Z_{1,2}| \approx 1$ (Fig. 2*C* and Movie S3). These synchronization modes correspond to the two eigenmodes of the swing/spring system. For intermediate κ, however, we observe chimeras (Fig. 2*B* and Movie S1). Whereas one of the metronome populations is fully synchronized with $|Z| \approx 1$, the other population is desynchronized. The trajectory of the order parameter of the desynchronized population describes a cloud in the complex plane with $|Z| < 1$. The phases of the desynchronized population are spread over the entire interval $[-\pi, \pi]$, and the time-averaged frequencies are nonidentical. As we increase κ, numerical simulations (see below) reveal that this cloud bifurcates off the AP mode, traverses the complex plane, and eventually collapses into the stable IP synchronization mode (see Fig. 4*B*). None of the metronomes in the desynchronized population is locked to the synchronized population either, demonstrating truly unlocked motion. Chimeras were consistently found for both SD and DS symmetries, ruling out chimeras as a result of asymmetry or pinning due to heterogeneities. Further, chimeras were not transient, such that the desynchronized population remained desynchronized (i.e., a DS or SD configuration remained for the entire duration of the experiment, typically lasting for up to 1,500 oscillation cycles).

Chimeras are sandwiched in a region between AP and IP modes consistently across various metronome frequencies (Fig. 3*A*). Remarkably, we also find other asynchronous states, including phase-clustered states (30) (Fig. S4); a "partial chimera," where only a fraction of the asynchronous population is frequency-locked; and states with oscillation death (28, 31). Additionally, we observe a region of bistability of chimeras and AP synchronized motion. Closer to the edge of the IP region, we find a narrow slice where neither of the metronome populations can achieve synchrony (DD state): Even when initialized with SD or DS conditions, the system loses synchrony completely after a transient time.

We have developed a mathematical model (*SI Text*, Fig. S5, and Table S1) that we simulated to corroborate our experimental findings and to test situations that cannot be achieved experimentally, such as large metronome populations or perfectly identical frequencies. The two swings are parametrized by their displacement angles from equilibrium positions, Φ and Ψ; the metronome pendula are parametrized by the displacement angles ϕ_i and ψ_i, respectively. The metronomes are described as self-sustained oscillators with (harmonic) eigenfrequency ω, damping μ_m with an amplitude-dependent nonlinearity $D(\phi_i)$ due to the escapement (28, 29, 31):

$$\ddot{\phi}_i + \sin\phi_i + \mu_m \dot{\phi}_i\, D(\phi_i) + \frac{\omega^2}{\Omega^2}\cos\phi_i\, \ddot{\Phi} = 0, \qquad [1]$$

where the terms represent (from left to right) pendulum inertia, gravitational force of restitution, damping, and the driving swing inertia, and the dots represent derivatives with respective to time

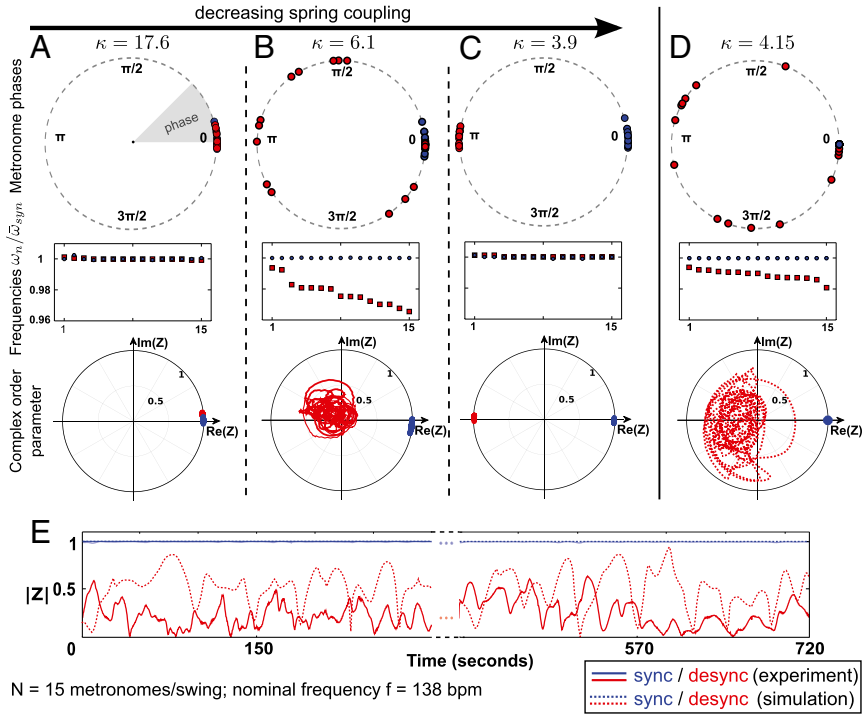

Fig. 2. Chimeras emerge with intermediate spring rate κ in a "competition" zone between two fully synchronous modes. With decreasing κ, we observe a transition from IP synchronization (*A*), over chimeras (*B*), to AP synchronization (*C*). The transition region also exhibits phase-clustered states and partial chimeras. (*D* and *E*) Simulations share all features of the experimental chimera. Data related to the synchronous and asynchronous populations are coded in blue and red, respectively. Angular frequencies are normalized with the average frequency of the synchronized population $\overline{\omega}_{syn}$. bpm, beats per minute.

$\tau = \omega t$. In turn, the swings of length L are described as harmonic oscillators with eigenfrequency $\Omega = \sqrt{g/L}$ and damping μ_s. A swing is driven by the metronomes and the neighboring swing, to which it is coupled with a spring of strength κ:

$$\ddot{\Phi} + \Omega^2\Phi - \kappa(\Psi - \Phi) + \mu_s\dot{\Phi} + \frac{x_0}{L}\sum_{k=1}^{N}\partial_{\tau\tau}\sin\phi_k = 0, \qquad [2]$$

where terms (from left to right) are swing inertia, force of restitution, spring coupling, friction, and the inertia summed over all metronomes on the same swing. Whereas κ determines the interpopulation coupling strength, the global coupling strength depends on the ratio of the metronome frequency and the swing eigenfrequency, $(\omega/\Omega)^2$. Using conditions similar to our experiments (but without frequency spread), chimeras obtained from simulations (Fig. 2 *D* and *E*) and the resulting phase diagram (Fig. 3*C*) agree qualitatively very well with experiments (quantitative differences are likely due to the ad hoc metronome model and potential discrepancies in parametrization as discussed in *SI Text* and Fig. S6). Bistability of fully synchronized (SS) and symmetry-breaking (SD and DS) states is a

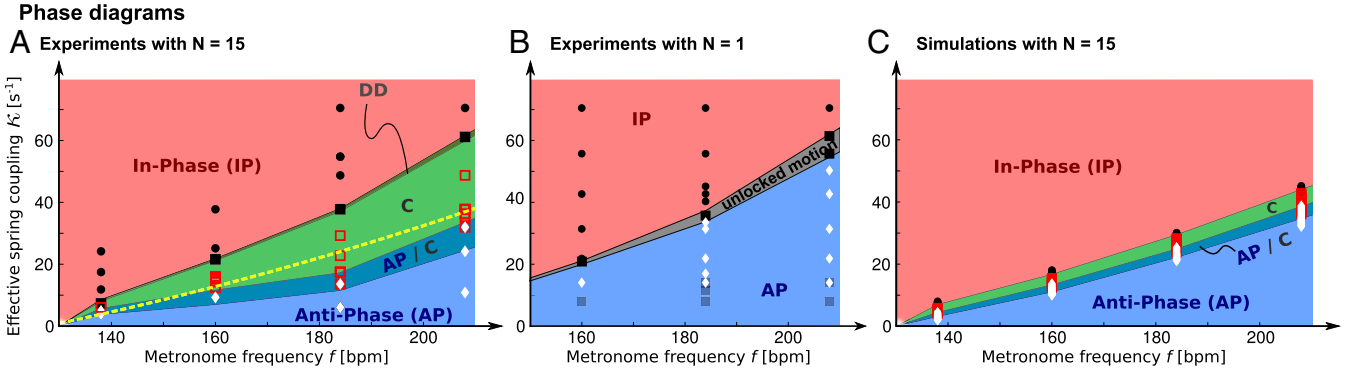

Fig. 3. Phase diagrams from experiments for $N = 15$ (*A*) and $N = 1$ (*B*) metronome(s) per swing and from numerical simulations with $N = 15$ metronomes (*C*) with metronome frequency f vs. effective spring coupling $\kappa = k/M(l/L)^2$. IP (red) and AP (blue) synchronization modes surround the chimera parameter region C (green) and the bistable AP/C region with chimeras and AP synchronization. Symbols represent data points (color shadings are guides only). Region C, centered around the resonance curve of the swings' AP mode (yellow dashed line) defined by $f \cdot \pi/60 = \sqrt{\Omega^2 + 2\kappa}$, exhibits chimeras and other partially synchronized states. The bistable region AP/C exhibits chimera-like and synchronized AP states; DD represents a region where neither population synchronizes fully. For $N = 1$, we find a similar region of unlocked motion, where the metronomes never synchronize. The phase diagram from numerical simulations for identical metronomes exhibits the same qualitative structure as the experiment, except that the width of region C is smaller (*SI Text*). Parameter space in experiments and simulations was sampled with varying spring coupling κ for metronome frequencies $f = 138$, $f = 160$, $f = 184$, and $f = 208$ bpm.

hallmark of the chimera instability (14), which is in distinct contrast to other symmetry-breaking scenarios mediated via supercritical transitions (13). It is therefore interesting to note that chimera states may coexist with AP synchronization modes in certain regions of the bifurcation diagram (Fig. 3 *A* and *C*).

Notably, when metronomes on each swing synchronize in an IP or AP mode, one envisages that the swings, together with the attached metronomes, collectively behave like two "giant" metronomes. These modes correspond to excitations of the eigenmodes of the swing pair with frequencies Ω (IP) and $\sqrt{2\kappa+\Omega^2}$ (AP). Indeed, for $N=1$ metronome per swing (Fig. 1*B*), we find that due to momentum transfer, the swing strictly follows the motion of the attached metronome pendulum: The system behaves like Huygens' experiment (i.e., with clocks replaced by metronomes). The metronomes settle into AP and IP synchronization modes for weak and strong coupling κ, respectively, as in modern reconstructions of Huygens' setup (31). Additionally, we find a small region where unlocked motion is possible (Fig. 3*B*).

Generalizing Huygens' experiment by adding internal degrees of freedom (i.e., metronomes) on each swing allows for much richer complex dynamics. A rich tapestry of complex states is uncovered (Fig. 4) in a transition from the AP to IP synchronization as the spring coupling κ is increased. In addition to chimeras, these include phase-clustered states (26): a "clustered chimera," where oscillators are attracted to a clustered state but cannot quite attain frequency locking; a partial chimera, where the asynchronous population appears partially locked; and a quasiperiodic chimera (17, 18). The situation is aptly captured by the notion of "more is different" (32): Additional internal degrees of freedom open a door to unexpected complex behavior [i.e., unanticipated by mere extrapolation of simple collective behavior (32)]. Using Huygens' term of the "odd sympathy of clocks" (1) to denote synchrony, the observed asymmetrical behavior might be described as an "antipathetic sympathy of clocks."

Chimeras and other partly synchronous states emerge as a competition in an intermediate regime between IP and AP synchronization modes: As a result, both modes are destroyed, such that only one of the giant metronomes wins the tug-of-war and remains synchronous, whereas the other one is broken apart. The resulting asymmetry is characterized by the domination of one giant over the other [i.e., the synchronous population forces the asynchronous population (33), acting like an energy sink]. Remarkably, we find that the parameter region with chimera-like behavior is centered around the resonance curve related to the swings' antiphase eigenmode (Fig. 3*A*): Near resonance, the fabric of uniform synchronization is torn.

Discussion

By devising a mechanical system composed of just two swings, a spring, and a number of metronomes (28), we have extended Huygen's original experiment (1, 31) and demonstrated how chimeras emerge in the framework of classical mechanics. Recent experiments (26, 27) could only produce chimeras by exploiting sophisticated computer-controlled feedback, and the time delay of the coupling had to be carefully crafted in addition to tuning its strength; by contrast, in our realization, chimeras emerge generically using merely a spring, without any need to adjust parameters other than the coupling strength. Notably, our setup is composed of basic mechanical elements, such as inertia, friction, and spring rate, which have exact or generalized analogs in other areas, such as electronic (6, 34), optomechanical (35), chemical (7), and icrobial systems or genetic circuits (36). The model we propose shows that the complex synchronization patterns found in the experiments are described by elementary dynamical processes that occur in diverse natural and technological settings. This raises the question of whether chimeras may have already been observed in such systems but remained unrecognized as such. For instance, our model equations translate directly to recent theoretical studies of synchronization in power grids (37–39) and optomechanical crystals (40, 41). Consequently, as power grid network topologies evolve to incorporate growing sources of renewable power, the resulting decentralized, hierarchical networks (37) may be threatened by chimera states, which could lead to large-scale partial blackouts and unexpected behavior. On the other hand, we envision that multistable patterns of synchrony and desynchrony (19) can be exploited to build on-chip memories

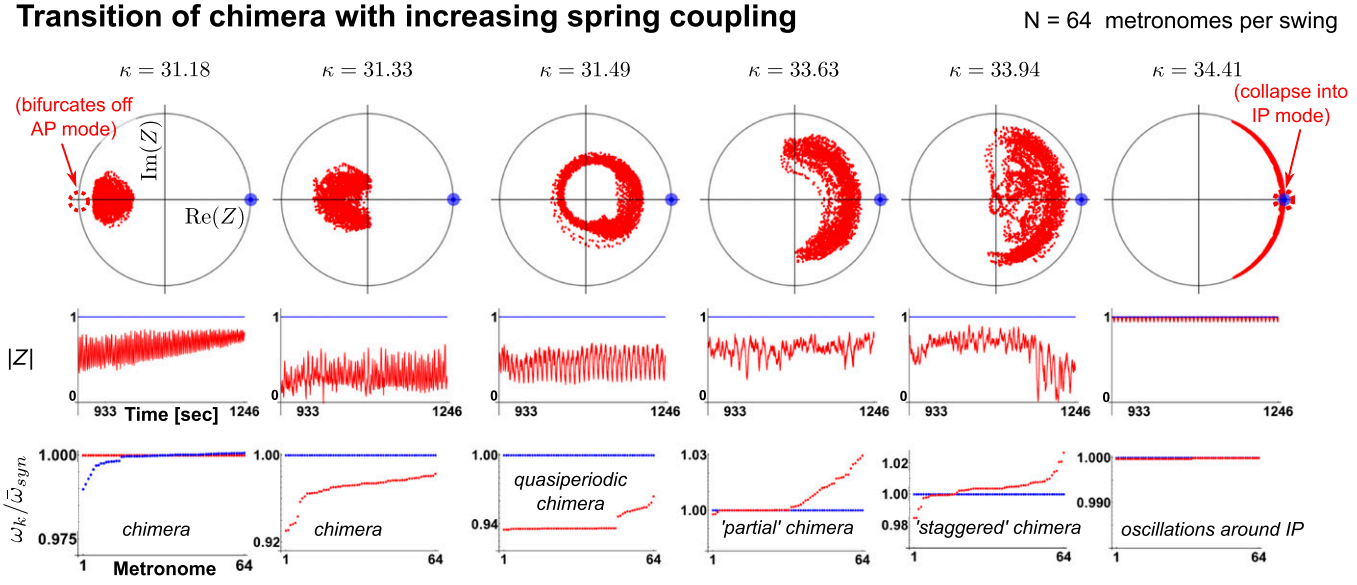

Fig. 4. Traversal of order parameter cloud with increasing spring coupling κ. A transition through a rich spectrum of chimera states becomes evident. Numerical simulations are carried out with $N=64$ metronomes (for parameters see *SI Text*). As κ increases, the complex order parameter Z_p bifurcates off from the AP mode at 180° and travels to the right, where it snaps into the IP synchronization mode at 0°. (*Top*) Complex order parameter Z is displayed. (*Middle*) Magnitude $|Z_p|$ is displayed. (*Bottom*) Angular frequencies, normalized with the average frequency of the synchronized population $\overline{\omega}_{\text{syn}}$, are displayed. The synchronized population is shown in blue, and the desynchronized population is shown in red.

and computers based on arrays of micromechanical devices (35). We expect the physical mechanisms that we uncovered here will have important and far-reaching ramifications in the design and use of such technologies and in understanding chimera states in nature.

Materials and Methods

Experiments. Two swings are suspended by four light hollow aluminum rods with a length of 50 cm (outer and inner diameters are 10 mm and 9 mm, respectively). The swings are attached to the rods via low-friction ball bearings to ensure smooth motion of the swings. The upper rod ends are attached in the same way on a large rigid support frame. The distance between the support frame and the board is set to $L = 22$ cm. The motion of the two swings is constrained so that it can occur, to high precision, only in the x-y plane. Each swing is made of a 500-mm × 600-mm × 1-mm perforated aluminum plate. The total weight of each plate is 915 ± 4 g. Each swing is loaded with $N = 15$ metronomes with a weight of 94 g. The total weight of the swing and metronomes is $M = 2.3$ kg. Two precision steel springs (Febrotec GmbH; spring constant $k = 34$ N/m) are firmly attached with clamps to the two adjacent swing rods (Fig. 1*A*) at a distance l above the pivot point. Adjusting the spring lever l changes the effective spring strength $\kappa = k/M(l/L)^2$. An experiment is started with a careful symmetry check of the system, by ensuring that the initial friction μ_s is the same on both swings. The metronome's nominal frequency is set to identical values ω_n. We then connect the two swings with the spring firmly set at a distance l above the pivot points. The motion of the metronomes and the swings is video-recorded under UV illumination using a Nikon D90 camera mounted with an 18- to 55-mm DX format lens. Each experiment is repeated with inverted roles of the swings (i.e., a DS experiment is followed by an SD experiment), such that the left-to-right symmetry is checked thoroughly.

Simulations. Simulations were carried out with identical metronomes until a stationary state was reached (typically, ~2,000 oscillation cycles). The phase diagram (Fig. 3*C*) was obtained by fixing the nominal metronome frequency f and then gradually increasing the effective spring rate κ (using similar parameters as in the experiment and $N = 15$ metronomes per swing). For each parameter step, synchronous IP and AP states were continued quasiadiabatically, whereas simulations resulting in chimera-like states were reinitialized with randomized phases in one of the populations (*SI Text*).

ACKNOWLEDGMENTS. We thank H. Stone, S. Strogatz, K. Showalter, A. Pikovsky, M. Rosenblum, S. Herminghaus, and L. Goehring for useful comments, and H. J. Martens for valuable discussions on the experimental design. We express deep gratitude to Udo Krafft for his assistance with the experimental setup. This work was partly supported by a grant from the Human Frontier Science Program (to S.T.).

1. Huygens C (1967) *Oeuvres complètes* (Swets & Zeitlinger Publishers, Amsterdam), Vol 15.
2. Michaels DC, Matyas EP, Jalife J (1987) Mechanisms of sinoatrial pacemaker synchronization: A new hypothesis. *Circ Res* 61(5):704–714.
3. Buck J, Buck E (1968) Mechanism of rhythmic synchronous flashing of fireflies. Fireflies of Southeast Asia may use anticipatory time-measuring in synchronizing their flashing. *Science* 159(3821):1319–1327.
4. Strogatz SH, Abrams DM, McRobie A, Eckhardt B, Ott E (2005) Theoretical mechanics: Crowd synchrony on the Millennium Bridge. *Nature* 438(7064):43–44.
5. Liu C, Weaver DR, Strogatz SH, Reppert SM (1997) Cellular construction of a circadian clock: Period determination in the suprachiasmatic nuclei. *Cell* 91(6):855–860.
6. Wiesenfeld K, Colet P, Strogatz S (1998) Frequency locking in Josephson arrays: Connection with the Kuramoto model. *Phys Rev E Stat Phys Plasmas Fluids Relat Interdiscip Topics* 57(2):1563–1569.
7. Kiss IZ, Zhai Y, Hudson JL (2002) Emerging coherence in a population of chemical oscillators. *Science* 296(5573):1676–1678.
8. Taylor AF, Tinsley MR, Wang F, Huang Z, Showalter K (2009) Dynamical quorum sensing and synchronization in large populations of chemical oscillators. *Science* 323(5914):614–617.
9. Danø S, Sørensen PG, Hynne F (1999) Sustained oscillations in living cells. *Nature* 402(6759):320–322.
10. Massie TM, Blasius B, Weithoff G, Gaedke U, Fussmann GF (2010) Cycles, phase synchronization, and entrainment in single-species phytoplankton populations. *Proc Natl Acad Sci USA* 107(9):4236–4241.
11. Motter AE (2010) Spontaneous synchrony breaking. *Nat Phys* 6(3):164–165.
12. Kuramoto Y, Battogtokh D (2002) Coexistence of coherence and incoherence in nonlocally coupled phase oscillators. *Nonlinear Phenomena in Complex Systems* 5(4):380–385.
13. Abrams DM, Strogatz SH (2004) Chimera states for coupled oscillators. *Phys Rev Lett* 93(17):174102.
14. Abrams DM, Mirollo R, Strogatz SH, Wiley DA (2008) Solvable model for chimera states of coupled oscillators. *Phys Rev Lett* 101(8):084103.
15. Montbrió E, Kurths J, Blasius B (2004) Synchronization of two interacting populations of oscillators. *Phys Rev E Stat Nonlin Soft Matter Phys* 70(5 Pt 2):056125.
16. Omel'chenko OE, Maistrenko YL, Tass PA (2008) Chimera states: The natural link between coherence and incoherence. *Phys Rev Lett* 100(4):044105.
17. Pikovsky A, Rosenblum M (2008) Partially integrable dynamics of hierarchical populations of coupled oscillators. *Phys Rev Lett* 101(26):264103.
18. Bordyugov G, Pikovsky A, Rosenblum M (2010) Self-emerging and turbulent chimeras in oscillator chains. *Phys Rev E Stat Nonlin Soft Matter Phys* 82(3 Pt 2):035205.
19. Martens EA (2010) Bistable chimera attractors on a triangular network of oscillator populations. *Phys Rev E Stat Nonlin Soft Matter Phys* 82(1 Pt 2):016216.
20. Martens EA, Laing CR, Strogatz SH (2010) Solvable model of spiral wave chimeras. *Phys Rev Lett* 104(4):044101.
21. Laing CR (2009) The dynamics of chimera states in heterogeneous Kuramoto networks. *Physica D* 238(16):1569–1588.
22. Laing CR, Rajendran K, Kevrekidis IG (2012) Chimeras in random non-complete networks of phase oscillators. Chaos: An interdisciplinary. *Journal of Nonlinear Science* 22(1):013132.
23. Olmi S, Politi A, Torcini A (2010) Collective chaos in pulse-coupled neural networks. *Europhys Lett* 92(6):60007.
24. Phillips JR, White J, Orlando TP, Orlando TP, van der Zant HS (1993) Influence of induced magnetic fields on the static properties of Josephson-junction arrays. *Phys Rev B Condens Matter* 47(9):5219–5229.
25. Swindale NV (1980) A model for the formation of ocular dominance stripes. *Proc R Soc Lond B Biol Sci* 208(1171):243–264.
26. Tinsley MR, Nkomo S, Showalter K (2012) Chimera and phase-cluster states in populations of coupled chemical oscillators. *Nat Phys* 8(8):662–665.
27. Hagerstrom AM, et al. (2012) Experimental observation of chimeras in coupled-map lattices. *Nat Phys* 8(8):658–661.
28. Pantaleone J (2002) Synchronization of metronomes. *Am J Phys* 70(10):992–1000.
29. Ulrichs H, Mann A, Parlitz U (2009) Synchronization and chaotic dynamics of coupled mechanical metronomes. *Chaos* 19(4):043120.
30. Golomb D, Hansel D, Shraiman B, Sompolinsky H (1992) Clustering in globally coupled phase oscillators. *Phys Rev A* 45(6):3516–3530.
31. Bennett M, Schatz M, Wiesenfeld K (2002) Huygen's clocks. *Proc R Soc Lond A Math Phys Sci* 458(2019):563–579.
32. Anderson PW (1972) More is different. *Science* 177(4047):393–396.
33. Childs LM, Strogatz SH (2008) Stability diagram for the forced Kuramoto model. *Chaos* 18(4):043128.
34. Temirbayev A, Zhanabaev Z, Tarasov S, Ponomarenko V, Rosenblum M (2012) Experiments on oscillator ensembles with global nonlinear coupling. *Phys Rev E Stat Nonlin Soft Matter Phys* 85(1 Pt 2):015204.
35. Zhang M, et al. (2012) Synchronization of micromechanical oscillators using light. *Phys Rev Lett* 109(23):233906.
36. Danino T, Mondragón-Palomino O, Tsimring L, Hasty J (2010) A synchronized quorum of genetic clocks. *Nature* 463(7279):326–330.
37. Rohden M, Sorge A, Timme M, Witthaut D (2012) Self-organized synchronization in decentralized power grids. *Phys Rev Lett* 109(6):064101.
38. Dörfler F, Chertkov M, Bullo F (2013) Synchronization in complex oscillator networks and smart grids. *Proc Natl Acad Sci USA* 110(6):2005–2010.
39. Motter AE, Myers SA, Anghel M, Nishikawa T (2013) Spontaneous synchrony in power-grid networks. *Nat Phys* 9(1):191–197.
40. Eichenfield M, Chan J, Camacho RM, Vahala KJ, Painter O (2009) Optomechanical crystals. *Nature* 462(7269):78–82.
41. Heinrich GH, Ludwig M, Qian J, Kubala B, Marquardt F (2011) Collective dynamics in optomechanical arrays. *Phys Rev Lett* 107(4):043603.